ChemPubSoc Europe

DOI: 10.1002/chem.201502062

CHEMISTRY A European Journal Full Paper

Analytical Methods

Rational Tuning of the Electrocatalytic Nanobiointerface for a "Turn-Off" Biofuel-Cell-Based Self-Powered Biosensor for p53 Protein

Yajing Han,[a] Johnny Muya Chabu,[a] Shengqiang Hu,[a] Liu Deng,*[a] You-Nian Liu,[a] and Shaojun Guo*[b]

Abstract: Herein, a novel tunable electrocatalytic nanobiointerface for the construction of a high-sensitivity and high-selectivity biofuel-cell (BFC)-based self-powered biosensor for the detection of transcription factor protein p53 is reported, in which bilirubin oxidase (BOD)/DNA supramolecular modified graphene/platinum nanoparticles hybrid nanosheet (GPNHN) works as a new enhanced material of biocathode to control the attachment of target, and thus tune the electron-transfer process of oxygen reduction for transducing signaling magnification. It is found that in the presence of p53, the strong interaction between the wild-type p53 and its consensus DNA sequence on the electrode surface can block the electron transfer from the BOD to the electrode, thus providing a good opportunity for reducing the electrocatalytic activity of oxygen reduction in the biocathode. This in combination with the glucose oxidation at the carbon nanotube/Meldola's blue/glucose dehydrogenase bioanode can result in a current/or power decrease of BFC in the presence of wild-type p53. The specially designed BFC-based self-powered p53 sensor shows a wide linear range from 1 pM to 1 μM with a detection limit of 1 pM for analyzing wild-type p53. Most importantly, our BFC-based self-powered sensors can detect the concentrations of wild-type p53 in normal and cancer cell lysates without any extensive sample pretreatment/separation or specialized instruments. The present BFC-based self-powered sensor can provide a simple, economical, sensitive, and rapid way for analyzing p53 protein in normal and cancer cells at clinical level, which shows great potential for creating the treatment modalities that capitalize on the concentration variation of the wild-type p53.

Introduction

The development of new-concept biosensors is of great importance in the areas of clinical diagnostics, forensic chemistry, food quality control and biological warfare detection, etc. Biofuel-cell (BFC)-based self-powered biosensors as a new class of devices, have attracted enormous research interest recently, by the use of an electrochemical energy transformation occurring in BFCs as a transducing element.[1–7] In principle, the biosensing concept based on BFCs can produce sufficient or insufficient energy for signaling in the presence of the analyte depending on putting more or less active biocatalyst of BFCs onto the electrode surface.[8–10] After the first BFC-based self-powered glucose sensors, several interesting sensing concepts based on BFCs have been developed to detect analytes such as glucose, ethanol and cellobiose, etc., that could be oxidized or reduced by a biological catalyst applied in BFCs.[11–14] Recently, by the use of inhibitor and decoupler effects, BFC-based self-powered sensing concepts have also be explored to detect other important analytes such as cyanide, ethylene diamine tetraacetic acid (EDTA) and explosive compounds.[4,9,10] These BFC-based sensors open the way for future point-of-care testing and might provide a helpful solution to low-cost and simple analytical systems without the need of any additional external energy. To date, the studies on BFC-based sensors mainly focus on their long-term operation, miniaturization, and extend the analytes scope. However, a few reports are focused on regulating/or tuning electrocatalytic processes at the electrode surface of BFCs,[15,16] which is the most fundamental factor for the development of BFC-based biosensors.

The design of highly efficient catalytic interfaces will be extremely important to tune the electrocatalytic process of BFC-based self-powered biosensors. Since the electrocatalytic process can be easily modulated by the outside analyte, thus affecting the output of BFCs, the quantitative recognition of the analyte can actually be realized by BFC-based biosensors. The switchable electrocatalytic interface for BFC-based sensors usually employ specific materials with tunable functions. These typical examples include monolayer photoisomer linked to bio-

[a] Y. Han, J. M. Chabu, S. Hu, Dr. L. Deng, Prof. Y.-N. Liu
College of Chemistry and Chemical Engineering
State Key Laboratory for Powder Metallurgy
Central South University, Changsha, Hunan, 410083 (P.R. China)
E-mail: dengliu@csu.edu.cn

[b] Prof. S. Guo
College of Engineering
Peking University, 100871 (P.R. China)
E-mail: shaojun.guo.nano@gmail.com

catalysts with photoswitchable bioelectrocatalytic processes,[17–19] and pH-sensitive redox polymer switched between the redox active and inactive states upon pH-induced swelling and shrinking processes,[20–23] etc. However, these developed switchable electrodes can only switch between the ON and OFF states with limited ability for sensor application. Recently, DNA has begun to be considered as a promising regulating element for tuning the electrocatalytic performance of enzyme on electrode surface. This is because different folding topologies and architecture of DNA can be achieved in the presence of metal ions[24–27] (such as Ag^+, K^+, or Pb^{2+}, etc.), complex nucleic acids or RNA, proteins or small molecules,[24,28,29] etc. These interesting structure transformations can result in electrochemical/or electrocatalytic process change on the electrode interface. This concept has been demonstrated in the use of aptamers (artificial DNA) to control the BFC output for the sensors.[2,30] However, the reported aptamer-based biochemical signals for controlling BFCs' power release can just realize a qualitative determination of the analytes. This can be ascribed to the little control over the molecular orientation in the above systems, which results in inefficient electron transfer and electrical contact. In order to solve the above issue related to electron transfer, recently researchers have focused on the introduction of mediator (e.g., ferrocene[31,32] and $[Os(2,2'\text{-bipyridine})_2Cl_2]^{2+/3+}$)[33–35] into the DNA-modified electrode interface for promoting electron transfer. However, these studies have their inherent disadvantages. Mediator-based electron transfer in biocatalysis processes is sophisticated, inconvenient and complex for the development of miniaturized sensors, since the mediator leak is unavoidable from the modified film. Thus, searching for effective, ingenious assembly of hybrid DNA/enzyme structures attached to nanomaterials modified electrode surface, that can precisely tune the electrocatalytic reaction of the enzyme and realize the rapid direct electron transfer (DET) between the enzyme and electrode, is very necessary for future high-performance BFC-based self-powered biosensors with high sensitivity and selectivity.

The common assay for p53 protein usually involves the use of p53 antibodies, which cannot distinguish the wild-type p53 and mutant p53,[45] or the electrophoretic mobility shift assay, which is semiquantitative at best. For clinical applications, it is always highly desirable to develop a simple, sensitive and selective quantitative method to detect p53. In this work, we demonstrate that a bilirubin oxidase (BOD)/DNA supramolecular assembly on graphene/platinum nanoparticles (NPs) hybrid nanosheet (GPNHN), can achieve DET-type electrocatalytic oxygen reduction for the biocathode of BFCs. Such interesting electrode interface can act as the transducing element for self-powered quantitative detection of p53. The interaction between p53 and DNA would block the electron transfer from the BOD to the electrode, thus leading to the decrease of oxygen reduction at the biocathode of BFCs. The decrease of output current at the cathode in combination with the glucose oxidation at the carbon nanotube/Meldola's blue/glucose dehydrogenase (CNT/MB/GDH) bioanode can result in a current/or power decrease that can be measured as the signal in the presence of wild-type p53. Our BFC-based self-powered p53 sensor shows a wide linear range from 1 pM to 1 μM with a detection limit of 1 pM for analyzing wild-type p53. To demonstrate the feasibility of this self-powered p53 biosensor in real samples, the detection of wild-type p53 in normal and cancer cells were carried out. The results determined by our method are consistent with previous ones, suggesting that it is amenable to the quantification of wild-type p53 levels in normal and cancer cells.

The schematic illustration on the BFC-based self-powered sensors for the detection of p53 is shown in Figure 1. First, to realize the DET-type biocathode, the electrochemical interface should provide a favorable microenvironment to maintain the enzyme activity and minimize the barrier of substrate and

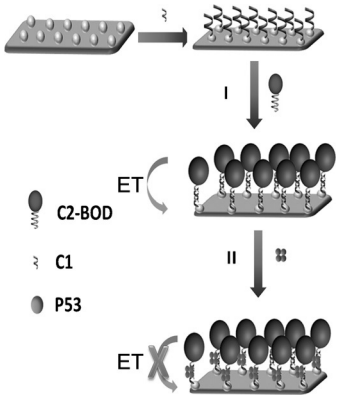

Figure 1. Schematic illustration of co-assembling the BOD/DNA duplex on GPNHN and also the sensing strategy of the BOD/DNA/GPNHN electrode for the detection of p53.

product. Herein, the as-prepared GPNHN was used to functionalize the indium-doped tin oxide (ITO) electrode for facilitating electron transfer between the redox sites of enzyme and the electrode. Then, the thiolated nucleic acid (C1) was assembled on GPNHN surface via SH–Pt interactions.[36,37] After that, the C1 on the GPNHN surface hybridized with its complementary C2, which was linked with BOD (Figure 1 I). The double stranded DNA duplex formed by C1 and C2 was able to act as the electrical wire to transfer the electron flow between the BOD and GPNHN. Then, the excellent conductivity of GPNHN provided a good opportunity for realizing the DET-type electrocatalysis of BOD (Figure 1 I). Both C1 and C2 include the DNA consensus site that can selectively bind wild-type p53. In the presence of wild-type p53, the DNA sequence can capture p53, thus blocking the electron transfer of BOD (Figure 1 II) and finally leading to the decreased the output of BFCs. As the concentration of p53 protein controls the extent of the electron transfer between the enzyme and electrode surface, the resulting bioelectrocatalytic currents are anticipated to correlate with the concentration of p53. Furthermore, since the formation of the DNA–p53 complex is coupled to a biocatalytic system, the quantitative analysis of p53 protein can be realized by the output decrease of the prepared BFCs.

Results and Discussion

GPNHN was facilely synthesized through heating a solution containing graphene oxide (GO), ascorbic acid (AA), Pt precursor and polyvinyl pyrrolidone (PVP) with the microwave-assisted heating method (see the details in the Experimental Section, Figure 2A). Herein, AA was used as a reducing agent for the effective reduction of both GO and Pt precursor. PVP worked as a stabilizing/linking agent for graphene and Pt NPs. The morphology and composition of GPNHN were studied by transmission electron microscopy (TEM) and X-ray photoelectron spectroscopy (XPS). Figure 2B and C shows the typical TEM images of GPNHNs at different magnifications. Many Pt NPs with the size of 3 nm are uniformly distributed on the surface of graphene. This is because the microwave system can provide a good microenvironment for the Pt nucleus, while the PVP can act as the stabilizer for Pt growth and also as an effective linker for the construction of GPNHN. The absence of isolated Pt NPs in the product reveals the strong link between graphene and Pt NPs. XPS patterns of the resulting GPNHN shows significant Pt 4f signals corresponding to the binding energy of Pt (Figure 2D) and significant C signal corresponding to the binding energy of graphene (Figure 2E), further supporting the conclusion that Pt NPs have been effectively assembled on the surface of graphene. The reduction of GO to graphene can also be characterized by XPS. The XPS spectrum of GO (Figure 2F) indicates the presence of two main types of carbon bonds: C–C (284.6 eV) and C–O (286.7 eV). After its reduction (Figure 2E), the peak associated with C–C (284.6 eV) becomes predominant, while the peaks related to the oxidized carbon species were greatly weakened. These results further indicate that GO has been well deoxygenated to form graphene, which is very important for improving its conductivity. It should be noted that herein the incorporation of Pt NPs on the graphene surface cannot only improve the electroactivity of the modified electrode, but also facilitate the immobilization of DNA sequence on the electrode by the SH–Pt interaction. Figure 2G depicts cyclic voltamogramms (CVs) of graphene (red line) and GPNHN (black line) in 0.5 M H_2SO_4 solution acquired at a scan rate of 50 mV s^{-1}. Hydrogen adsorption/desorption and oxide formation/reduction regions of Pt are obviously observed in GPNHN, indicating that Pt NPs have been effectively loaded on the graphene.

The electrochemical performance of the co-assembly of BOD and DNA duplex on GPNHN-modified ITO electrode was examined by its ability to reduce oxygen. Figure 3A shows CVs of

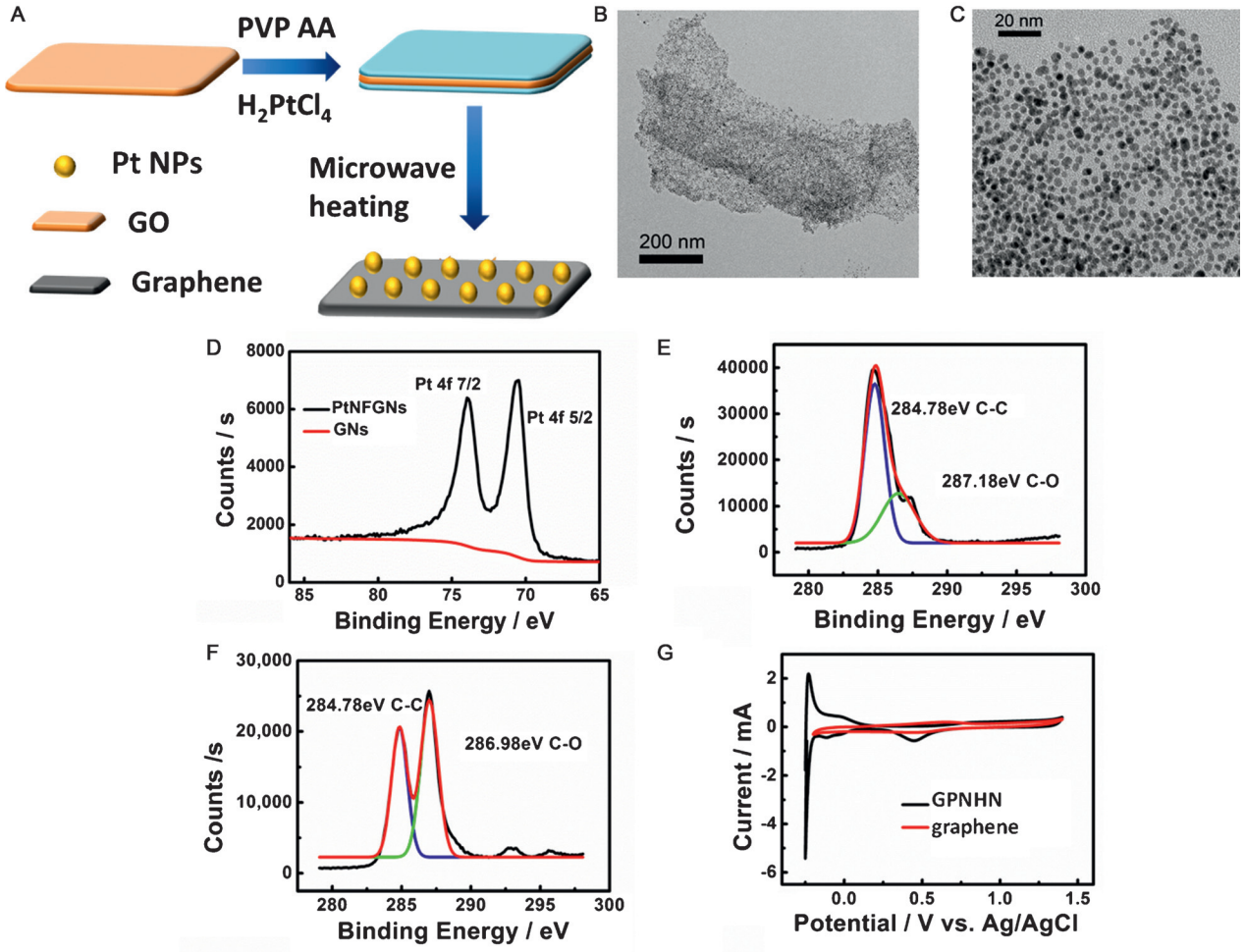

Figure 2. A) Schematic illustration of the synthesis of the GPNHN. B, C) TEM images of the GPNHN at different magnifications. XPS spectra of: D) Pt, and E) C in the GPNHN. F) XPS spectrum of C in grapheme oxide. G) CVs of the GPNHN (black) and graphene (red) in a 0.5 M H_2SO_4 solution.

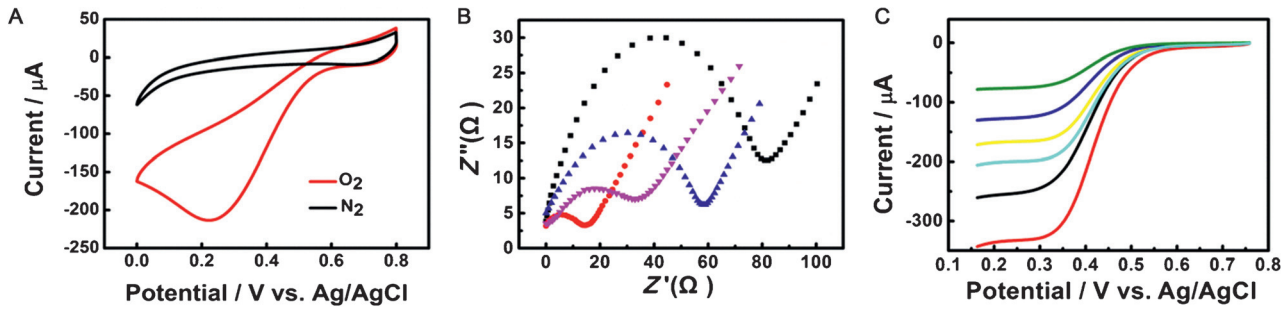

Figure 3. A) CVs of BOD/DNA/GPNHN/ITO electrode in nitrogen-saturated (black) and oxygen-saturated (red) 0.1 M PBS (pH 7.2) solution. B) EIS of BOD/DNA/GPNHN/ITO electrode in the presence of 0 M (red), 10 pM (magenta), 1 nM (blue) and 1 μM (black) p53. C) The polarization curves of BOD/DNA/GPNHN/ITO electrode in oxygen-saturated solution in the presence of 0 M (red), 10 pM (black), 50 pM (cyan), 100 pM (yellow), 200 pM (blue) and 500 pM (green).

BOD/DNA/GPNHN/ITO electrode in a nitrogen-saturated (black) and air-saturated (red line) 0.1 M phosphate buffer solution (PBS) (pH 7.5). The BOD/DNA/GPNHN/ITO electrode produces a large cathodic wave in the absence of mediator. Upon hybridization, the C2-sequence attached BOD was electrically wired by the DNA duplex, allowing electron transfer from the redox site of BOD to GPNHN. We found that the BOD/DNA/GPNHN/ITO electrode does not produce an observable redox response under anaerobic condition. The O_2 reduction commences at 0.58 V versus Ag/AgCl (0.78 V vs. the normal hydrogen electrode (NHE)) on BOD/DNA/GPNHN electrode, which is the same as the redox potential of the Cu ion at the type 1 Cu site of BOD (0.78 V vs. NHE). These results indicate that BOD wired by the DNA duplex to the GPNHN can work as an efficient DET-type biocatalyst for O_2 reduction, suggesting an effective electron transfer through the DNA wire and the low over-potential required for O_2 reduction at the as-prepared BOD/DNA/GPNHN/ITO electrode.

The level of p53 protein can increase in response to damaged DNA, and over 50% of human cancer cases contain mutations in p53.[40,41] Thus, due to its physiological significance, herein, we take p53 protein as the model target of our new self-powered sensor. As is known, the wild-type p53 protein is capable of highly selectively binding to the consensus-site DNA.[45] When exposing the BOD/DNA/GPNHN/ITO electrode to p53, p53 can readily tetramerize via the C termini,[42] and the resultant p53 tetramer can bind to the double-stranded DNA consensus site. Thus, the biocatalytic O_2 reduction process obviously reduces on p53/BOD/DNA/GPNHN/ITO electrode, due to the binding of p53 to the DNA sequence, producing the reduced electron transfer and high resistance. This recognition of p53 by BOD/DNA/GPNHN/ITO electrode was first monitored by electrochemical impedance spectroscopy (EIS) of BOD/DNA/GPNHN/ITO towards different concentration of p53. As shown in Figure 3B, the R_{et} response increases with increasing the p53 concentration, indicating that the p53 protein binds to the DNA consensus site, resulting in the reduced electron transfer path along the DNA sequence between the BOD and GPNHN. The more the p53 tretramers are linked, the slower the electron transfer rate is. The polarization curves of BOD/DNA/GPNHN/ITO electrode for oxygen reduction in the presence of p53 with different concentrations show that the polarization current decreases with increasing the amount of target (p53; Figure 3C), being in accord with the above EIS result. Therefore, the interaction between the p53 and DNA is able to control the electrical flow existing between the enzyme and electrode, thus leading to rationally tune the bioelectrocatalytic current of oxygen, correlating with the concentration of p53.

The CNT/MB/GDH/ITO electrode was applied as bioanode for achieving glucose electro-oxidation. Figure 4A shows the polarization curves of the CNT/MB/GDH modified anode (red curve) and the BOD/DNA/GPNHN cathode (black curve) in 20 mM PBS (pH 7.5) containing 5 mM NAD^+ and 15 mM glucose solution in air. The onset potential for the electro-oxidation of glucose is observed at −0.1 V, and the peak current density can reach a plateau at 240 $\mu A\,cm^{-2}$ at approximately 0.2 V. The onset potential for the electroreduction of O_2 is observed at +0.51 V and the current density reached a plateau with 275 $\mu A\,cm^{-2}$ at approximately 0.1 V. These results show excellent biocatalytic activities of both bioanode and biocathode, and make it possible to assemble a compartment-less glucose/O_2 BFCs in this study. A compartment-less glucose/O_2 BFC was assembled according to previous protocols.[10] Figure 4B displays the power curve of the assembled glucose/O_2 BFCs in a pH 7.5 (0.14 M NaCl + 0.02 M PBS) with a quiescent 5 mM NAD^+, 15 mM glucose solution in the air. The open circuit voltage (V_{oc}) of the cell is estimated to be 625 mV (relative standard deviation (RSD) = 0.7%, $n = 8$) and the maximum power density (P_{max}) reaches 378 $\mu W\,cm^{-2}$ at 392 mV (RSD = 1.3%, $n = 8$).

Under the optimal conditions, our BFC-based self-powered sensing platform was used to quantitatively detect wild-type p53 protein. First, the BOD/DNA/GPNHN biocathode was reacted with a series concentration of wild-type p53 to obtain the different outputs of BFCs. Figure 5A shows the current–voltage curves of the as-prepared BFCs in the presence of p53 with various concentrations. It is observed that the maximum current (I_{max}) values of the cell decreases with increasing the P53 concentration. As shown in Figure 5B, there is a linear relationship between ΔI_{max} (the different I_{max} value between non-p53 and target p53) and p53 concentration from 1 pM to 1 μM ($R^2 = 0.999$) with a detection limit of 1 pM, which is tenfold lower than that of the immnosandwich electrochemical sensor for p53 based on GO as a nanocarrier in a multienzyme amplification strategy,[43] and about two times lower than that of electrochemical p53 sensor using gold NP/ferrocene as the

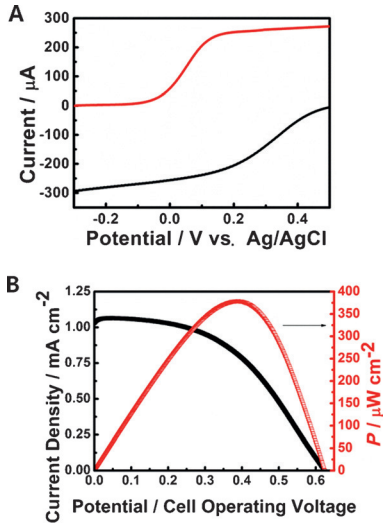

Figure 4. A) The polarization curves of the CNT/MB/GDH bioanode and BOD/DNA/GPNHN biocathode in air-saturated quiescent 0.02 M PBS (pH 7.5) containing 5 mM NAD^+ and 15 mM glucose solution. B) The current–potential (black) and polarization curves (red) of the assembled BFCs in air-saturated quiescent 0.14 M NaCl + 0.02 M PBS (pH 7.5) containing 5 mM NAD^+ and 15 mM glucose solution.

probe.[44]. Figure 5C shows the selectivity of our self-powered P53 sensor by the use of B-cell lymphoma 2 (Bcl-2), bovine serum albumin (BSA), and human serum albumin (HSA) as interfering agents. The results show that these interfering agents lead to almost no signal change, thus the selectivity is satisfactory. The reproducibility of our BFC-based self-powered sensor was examined by detecting 1 nM p53 with five different sensors. The relative standard deviation (RSD), estimated from the slopes of the calibration plots of five different and freshly prepared p53 sensors, was 7.6%, suggesting the good precision and reproducibility of our self-powered sensor.

Herein, to demonstrate the feasibility of practical detection, the as-prepared self-powered BFC-based sensors were used to analyze p53 in real samples. Figure 5D shows the polarization curves of the as-prepared BFC-based sensors in the presence of wild-type p53 from normal epithelial kidney cell 293T lysates (red) and lung adenocarcinoma cell A549 lysates (black). The p53 concentration level can be determined to be 3.467(±0.039) nM in normal epithelial kidney cell lysates, and 0.013(±0.004) nM in colorectal cancer cell lysates. This suggests that the p53 gene had been severely mutated in the colorectal cancer cells. To further establish the validity of this method for clinical applications, we also measured five additional cell lysate samples. Among the total five cancer cell-lines (leukemia cell K562, lung cancer cell A549, colorectal cancer cell HT29, brain tumor cell SF767 and cervical cancer cell Hela229), they all display substantially (50–260 times) lower wild-type p53 concentration than those in the normal cell lysates (normal kidney cell 293T and HEK293; Table 1). An obvious decline of the wild-type p53 concentration is ascribed to the elevation of the mutant p53 concentration, which usually occurs in cancer cells. Furthermore, our data in Table 1 are highly consistent with those determined with previous methods.[44] Therefore, our self-powered BFC-based p53 biosensor is amenable to the quantification of wild-type l p53 levels in normal and cancer cells.

Table 1. The determination of wild-type p53 concentrations in normal cell lysates and cancer cell lysates.

Cell lysates	wild-type p53 concentration [nM]
normal epithelial kidney cell 293T	3.467 ± 0.039
normal embryonic kidney cell HEK293	5.665 ± 0.053
leukemia cell K562	0.066 ± 0.007
lung adenocarcinoma cell A549	0.013 ± 0.0004
colorectal cancer cell HT29	0.028 ± 0.010
brain tumor cell SF767	0.106 ± 0.027
cervical carcinoma cell HeLa229	0.041 ± 0.015

Conclusions

To summarize, we have for the first time developed a label-free, BFC-based self-powered biosensor for the detection of

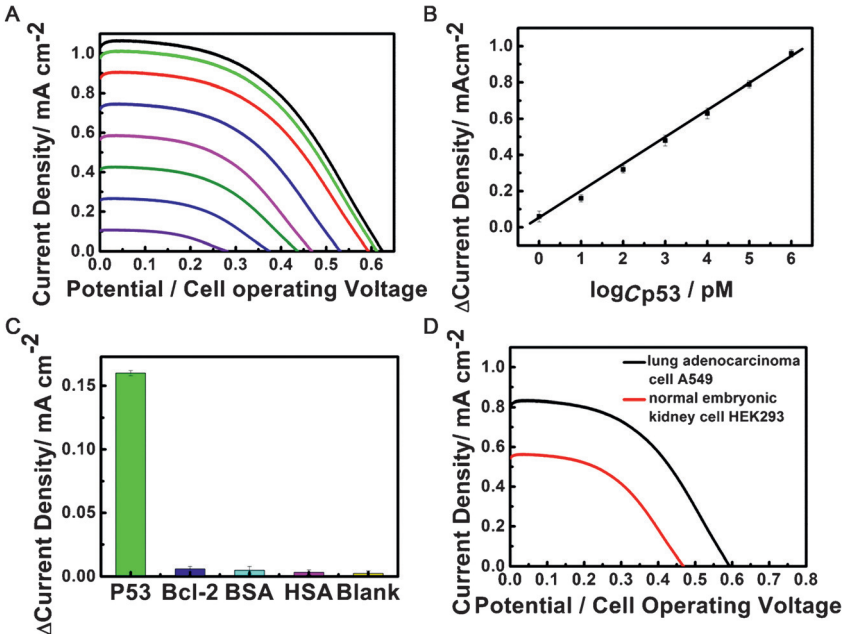

Figure 5. A) The current–potential curve of the disposable BFCs towards different concentration of p53: 0 M (black), 1 pM (green), 10 pM (red), 100 pM (blue), 1 nM (magenta), 10 nM (dark green), 100 nM (dark blue), 1 μM (purple). B) The linearity between the ΔI_{max} and the concentration of p53. C) The selectivity of disposable BFC-based self-powered sensor towards p53 (10 pM), Bcl-2 (10 nM), BSA (10 nM) and HSA (10 nM). D) The current–potential curve of the disposable BFC-based self-powered sensors towards normal epithelial kidney cell 293T lysates (red) and lung adenocarcinoma cell A549 lysates (black).

wild-type p53 with high sensitivity and selectivity. The DNA and BOD co-modified GPNHN were employed as a conducting matrix for facilitating the electrical contact between the BOD and electrode. This is very important for realizing the DET-type bioelectrocatalytic reduction of oxygen. Because the recognition of wild-type p53 to the consensus DNA site is coupled to the above biocatalytic system, the recognition of p53 is amplified by the rationally designed bioelectrocatalytic interface. Such an interesting biocathode combined with CNTs/MB/GDH film bioanode can result in a compartment-less glucose/O_2 BFCs with a V_{oc} of 625 mV and maximum power density of 378 $\mu W cm^{-2}$, which can further work as a self-powered sensor for the detection of p53. It is interestingly found that our self-powered p53 sensor shows a wide linear range from 1 pM to 1 μM with a very low detection limit of 1 pM for analyzing the wild-type p53. The implementation of the prepared self-powered sensor to real sample analysis has been demonstrated by determining wild-type p53 from normal and cancer cell lysates. The concentrations of wild-type p53 in normal and cancer cell lysates were successfully detected without any extensive sample pretreatment/separation or specialized instruments. The results showed that all the five cancer cell-lines have substantially (50–260 times) lower wild-type p53 concentration than the normal cell lysates. Most notably, the present self-powered BFC-based sensor can be accomplished only with a multimeter without the need of any expensive and large instruments, and provides a simple, economical, sensitive, and rapid process for assaying p53 protein in normal and cancer cells at clinical level.

Experimental Section

Reagents and materials

CNTs were purchased from Shenzhen Nanotech Port Co. Ltd. (NTP, China), and further treated with a mixed acid of HNO_3 and H_2SO_4 to obtain COOH groups on their surface. Graphene oxide (GO) was synthesized from graphite (Afar Aster) by a modified Hummers method.[38] Tris-(hydroxymethyl)aminomethane hydrochloride (Tris-HCl), 1-hexanethiol (HT), H_2PtCl_6, bilirubin oxidase (BOD) from *Myrothecium verrucaria*, 1-ethyl-3-(3-dimethyllaminopropyl)carbodiimide hydrochloride (EDC), *N*-hydroxysuccinimide (NHS), dithiothreitol (DTT), KH_2PO_4 and K_2HPO_4 were purchased from Sigma–Aldrich. PVP·K30 (M_w = 30000–40000) and ascorbic acid (AA) were obtained from Beijing Chemical Reagent Company (Beijing, China). Recombinant p53 sample was purchased from BD Biosciences Pharmingen (San Diego, CA). The oligonucleotides were purchased from Shanghai Sangon Biological Engineering Co. Ltd. (China). Their sequences are as follows:

C1: 5′-HS$(CH_2)_6$-TTT TTG GGC ATG TCT GGG CAT GTC T-3′

C2: 5′-$H_2N(CH2)_6$-TTT TTT AGA CAT GCC CAG ACATGC CC-3′

The p53 in normal and cancer cell lysates was obtained from Xiangya Hospital. Other reagents were all from commercial sources with analytical purity and used as received. All stock solutions were prepared daily with deionized water was treated with a water purification system (Simplicity 185, Millipore Corp., Billerica, MA).

Instruments

The electrochemical measurements of bioelectrodes were performed using a CHI832C (Shanghai Chenhua). Coiled platinum wire and an Ag/AgCl (saturated KCl) electrode were used as the counter electrode and the reference electrode, respectively. Current and potential output of the BFC system was measured by using a digital multimeter (Keithley 2700). We connected the two electrodes through an external 50 Ω resistor for the assessment of the BFCs performance. All tests were conducted at room temperature. Transmission electron microscopy (TEM) images were obtained with a Hitachi H-600 microscope (Japan).

Synthesis of GPNHN

GO solution (2 mL of 1 $mg mL^{-1}$ solution), 1 mL of 1 M PVP solution and 6 mL of 0.2 M AA solution was added into 12 mL water. After being immediately sonicated for about 2 min, 2 mL 0.1 M H_2PtCl_6 solution was added into the above mixture, followed by microwave oven treatment for 90 s (power: 800 W). The product was isolated by centrifugation at 8000 rpm for 15 min, followed by consecutive washing/centrifugation cycles three times with water. The collected product was redispersed in water/ethanol mixture (8 mL) with sonication to produce a colloidal suspension.

Preparation of C2-BOD bioconjugate

5′-Amine-terminated C2 (30 μL of 1 μM solution) was first treated with 10 μL of freshly prepared 0.4 M EDC and 0.1 M NHS solution for 30 min. Then, 10 μL of the BOD solution (1 $mg mL^{-1}$ in PBS) was added into the above mixture, and further allowed to react for 45 min. After further dialysis treatment, overnight, at 4 °C to remove the excess ingredient, the solution was diluted with PBS buffer and immediately stored at 4 °C before use.

Fabrication of the biocathode

The ITO electrode was thoroughly cleaned before use. An aliquot (5 μL) of the GPNHN (1 $mg mL^{-1}$) was first dropped onto ITO electrode. After being dried, 10 μL of TE (10 mM Tris-HCl and 1.0 mM EDTA) solution containing 1.0 μM C1 was cast onto the electrode, overnight, to immobilize the thiolated C1. This step was followed by washing the electrode thoroughly with water and soaking the electrode in an aqueous solution containing 0.1 mM HT for 5 min. To form the co-assembly of BOD and DNA duplex on GPNHN surface, 5.0 μL of TNE (TE + 0.02 M $MgCl_2$) comprising a predetermined concentration of C2-BOD was cast onto the electrode premodified with a C1/GPNHN surface. Then, the hybridization reaction was allowed to proceed for 2 h at room temperature. Finally, the BOD/DNA/GPNHN/ITO electrode was cleaned thoroughly with TNE solution. For the p53 protein capture, 5 μL of p53 solution at a given concentration was dropped onto the electrode surface and further incubated for 1 h. Finally, the p53/BOD/DNA/GPNHN/ITO electrode was rinsed with the washing buffer and water.

Fabrication of the bioanode

The CNT/MB/GDH/ITO electrode was prepared as reported with a slight modification.[39] An aliquot (10 μL) of 2 $mg mL^{-1}$ CNTs water solution was dropped onto a clean ITO electrode, dried with the droplet and rinsed with distilled water. GDH was adsorbed onto CNTs/ITO, overnight (4 °C), by casting 5 μL GDH (10 $mg mL^{-1}$) solution on the CNTs/ITO electrode surface, followed by further immersion of the modified electrode into MB solution for 30 min. Please note that rinsing the above modified electrode into doubly dis-

tilled water was necessary to remove the loosely bound dye/enzyme molecules for each modification step. Finally, the enzyme electrode was cross-linked with glutaraldehyde (as CNT/MB/GDH/ITO).

Fabrication of BFCs

The above CNT/MB/GDH and the BOD/DNA/GPNHN modified ITO electrodes acted as the bioanode biocathode, respectively, for the assembly of a glucose/O_2 BFC.

The ITO chip electrode was fabricated with the same protocol as previously reported.[12] The chips containing the electrodes were prepared using standard microfabrication on ITO glass plates. Two electrodes with surface size as 5 mm×5 mm were etched on the ITO surface. All modification processes were carried out in a PDMS cell with 5 mm×5 mm (the same size as the electrode surface)× 60 mm (height). Then we constructed a miniature BFC by the use of bioanode and biocathode prepared according to the above-mentioned method. Then a PDMS flow cell with dimensions of 10 mm×10 mm×60 mm covered the two modified electrodes. After that, the electrolyte was added into the cell to generate the power output. A 0.14 M NaCl+20 mM PBS (pH 7.5) containing 5 mM NAD^+ and 15 mM glucose solution was used as fuel solution.

Microchip-based BFCs for detection of p53

To detect p53 or other proteins, 5 μL of PBS containing a given concentration of p53 or other proteins was cast onto the cathode surface for 1 h, followed by washing in PBS. Here, the p53 concentration was calculated by the molecular mass of the p53 monomer. The circuit *V–I* curves were recorded in 0.14 M NaCl+20 mM PBS (pH 7.5) containing 5 mM NAD^+ and 15 mM glucose in air. To evaluate the applications of the proposed self-powered sensor, normal and cancer cell lysates containing p53 were collected from the Xiangya Hospital. These cell lysates samples (10 μL) were directly added into the cathode chamber for p53 capture, followed by washing in PBS.

Acknowledgements

We are grateful to the National Natural Science Foundation of China (Nos. 21105126, 21076232 and 21276285) for support.

Keywords: analytical methods · biofuel cell · biosensors · DNA–protein interactions · tunable electrochemical interface

[1] A. Zebda, C. Gondran, A. Le Goff, M. Holzinger, P. Cinquin, S. Cosnier, *Nat. Commun.* **2011**, *2*, 370 – 375.
[2] M. Zhou, Y. Du, C. G. Chen, B. L. Li, D. Wen, S. J. Dong, E. K. Wang, *J. Am. Chem. Soc.* **2010**, *132*, 2172 – 2174.
[3] T. Miyake, S. Yoshino, T. Yamada, K. Hata, M. Nishizawa, *J. Am. Chem. Soc.* **2011**, *133*, 5129 – 5134.
[4] M. N. Germain, R. L. Arechederra, S. D. Minteer, *J. Am. Chem. Soc.* **2008**, *130*, 15272 – 15274.
[5] M. Zhou, N. D. Zhou, F. Kuralay, J. R. Windmiller, S. Parkhomovsky, G. Valdes-Ramirez, E. Katz, J. Wang, *Angew. Chem. Int. Ed.* **2012**, *51*, 2686 – 2689; *Angew. Chem.* **2012**, *124*, 2740 – 2743.
[6] L. Bai, L. H. Jin, L. Han, S. J. Dong, *Energy Environ. Sci.* **2013**, *6*, 3015 – 3021.
[7] L. Han, L. Bai, S. J. Dong, *Chem. Commun.* **2014**, *50*, 802 – 804.
[8] Y. H. Wang, L. Ge, P. P. Wang, M. Yan, J. H. Yu, S. G. Ge, *Chem. Commun.* **2014**, *50*, 1947 – 1949.
[9] L. L. Zhang, M. Dong, S. J. Zhou, *Anal. Chem.* **2012**, *84*, 10345 – 10349.
[10] L. Deng, C. G. Chen, M. Zhou, S. J. Guo, E. K. Wang, S. J. Dong, *Anal. Chem.* **2010**, *82*, 4283 – 4287.
[11] E. Katz, A. F. Bückmann, I. Willner, *J. Am. Chem. Soc.* **2001**, *123*, 10752 – 10753.
[12] A. Zloczewska, A. Celebanska, K. Szot, D. Tomaszewska, M. Opallo, M. Jonsson-Niedziolka, *Biosens. Bioelectron.* **2014**, *54*, 455 – 461.
[13] Z. H. Liu, B. Cho, T. M. Ouyang, B. Feldman, *Anal. Chem.* **2012**, *84*, 3403 – 3409.
[14] H. J. Cheng, P. Yu, X. L. Lu, Y. Q. Lin, T. Ohsaka, L. Q. Mao, *Analyst* **2013**, *138*, 179 – 185.
[15] D. L. Guan, Y. Kurra, W. S. Liu, Z. L. Chen, *Chem. Commun.* **2015**, *51*, 2522 – 2525.
[16] L. Amir, S. A. Carnally, J. Rayo, S. Rosenne, S. M. Yerushalmi, O. Schlesinger, M. M. Meijler, L. Alfonta, *J. Am. Chem. Soc.* **2013**, *135*, 70 – 73.
[17] A. Efrati, O. Yehezkeli, R. T. El-Vered, D. Michaeli, R. Nechushtai, I. Willner, *ACS Nano* **2012**, *6*, 9258 – 9266.
[18] T. Niazov, B. Shlyahovsky, I. Willner, *J. Am. Chem. Soc.* **2007**, *129*, 6374 – 6375.
[19] G. Fioravanti, N. Haraszkiewicz, E. R. Kay, S. M. Mendoza, C. Bruno, M. Marcaccio, P. G. Wiering, F. Paolucci, P. Rudolf, A. M. Brouwer, *J. Am. Chem. Soc.* **2008**, *130*, 2593 – 2601.
[20] M. Motornov, R. Sheparovych, E. Katz, S. Minko, *ACS Nano* **2008**, *2*, 41 – 52.
[21] L. Amir, T. K. Tam, M. Pita, M. M. Meijler, L. Alfonta, E. Katz, *J. Am. Chem. Soc.* **2009**, *131*, 826 – 832.
[22] M. Privman, T. K. Tam, M. Pita, E. Katz, *J. Am. Chem. Soc.* **2009**, *131*, 1314 – 1321.
[23] T. K. Tam, J. Zhou, M. Pita, M. Ornatska, S. Minko, E. Katz, *J. Am. Chem. Soc.* **2008**, *130*, 10888 – 10889.
[24] F. Wang, C. H. Lu, I. Willner, *Chem. Rev.* **2014**, *114*, 2881 – 2941.
[25] J. Liu, Y. A. Lu, *J. Am. Chem. Soc.* **2003**, *125*, 6642 – 6643.
[26] B. R. Baker, R. Y. Lai, M. S. zWood, E. H. Doctor, A. J. Heeger, K. W. Plaxco, *J. Am. Chem. Soc.* **2006**, *128*, 3138 – 3139.
[27] M. Hollenstein, C. Hipolito, C. Lam, D. Dietrich, D. M. Perrin, *Angew. Chem. Int. Ed.* **2008**, *47*, 4346 – 4350; *Angew. Chem.* **2008**, *120*, 4418 – 4422.
[28] Y. Xiao, A. A. Lubin, A. J. Heeger, K. W. Plaxco, *Angew. Chem. Int. Ed.* **2005**, *44*, 5456 – 5459; *Angew. Chem.* **2005**, *117*, 5592 – 5595.
[29] J. Liu, Y. Lu, *Angew. Chem. Int. Ed.* **2007**, *46*, 7587 – 7590; *Angew. Chem.* **2007**, *119*, 7731 – 7734.
[30] M. Zhou, X. Zheng, J. Wang, S. A. Dong, *Chem. Eur. J.* **2010**, *16*, 7719 – 7724.
[31] G. Piperberg, O. I. Wilner, O. Yehezkeli, R. Tel-Vered, I. Willner, *J. Am. Chem. Soc.* **2009**, *131*, 8724 – 8725.
[32] G. Mor-Piperberg, R. Tel-Vered, J. Elbaz, I. Willner, *J. Am. Chem. Soc.* **2010**, *132*, 6878 – 6879.
[33] Y. Zhang, A. Pothukuchy, W. Shin, Y. Kim, A. Heller, *Anal. Chem.* **2004**, *76*, 4093 – 4097.
[34] Y. Zhang, H.-H. Kim, A. Heller, *Anal. Chem.* **2003**, *75*, 3267 – 3269.
[35] H.-H. Kim, Y. Zhang, A. Heller, *Anal. Chem.* **2004**, *76*, 2411 – 2414.
[36] T. Laiho, J. Leiro, J. Lukkari, *Appl. Surf. Sci.* **2003**, *212*, 525 – 529.
[37] S. E. Eklund, D. E. Cliffel, *Langmuir* **2004**, *20*, 6012 – 6018.
[38] W. Hummers, R. J. Offeman, *J. Am. Chem. Soc.* **1958**, *80*, 1339 – 1342.
[39] D. Wen, L. Deng, S. J. Guo, S. J. Dong, *Anal. Chem.* **2011**, *83*, 3968 – 3972.
[40] S. J. Baker, S. Markowitz, E. R. Fearon, J. Willson, B. Vogelstein, *Science* **1990**, *249*, 912 – 915.
[41] E. Yonish-Rouach, D. Resnftzky, J. Lotem, L. Sachs, A. Kimchi, M. Oren, *Nature* **1991**, *352*, 345 – 347.
[42] J. Balintová, J. Špaček, R. Pohl, M, Brázdová, L. Havran, M. Fojta, M. Hocek, *Chem. Sci.* **2015**, *6*, 575 – 579.
[43] D. Du, L. Wang, Y. Shao, J. Wang, M. H. Engelhard, Y. Lin, *Anal. Chem.* **2011**, *83*, 746 – 752.
[44] J. Wang, X. Zhu, Q. Tu, Q. Guo, C. S. Zarui, J. Momand, X. Z. Sun, F. Zhou, *Anal. Chem.* **2008**, *80*, 769 – 774.
[45] J. Wölcke, M. Reimann, M. Klumpp, T. Göhler, E. Kim, W. Deppert, *J. Biol. Chem.* **2003**, *278*, 32587 – 32595.

Received: May 27, 2015
Published online on July 23, 2015